Responses to Referee #1's comments

Manuscript number: egusphere-2024-3841
Full title: Assessment of horizontally-oriented ice crystals with a combination of multiangle polarization lidar and cloud Doppler radar Author(s): Wu Z. et al.

The authors proposed and performed a novel retrieval process to infer the horizontally oriented ice crystals (HOIC) using ground-based Doppler radar, zenith-pointing polarimetric lidar, and 15° off zenith-pointing polarimetric lidar. A combination of zenith-pointing and off-zenith-pointing lidars can provide range-resolved detections of HOICs in ice or mixed-phase clouds. The case study demonstrates a distinct relation between the abundance of HOICs and eddy dissipation rates inferred from collocated Doppler radar. In addition, correlations between HOICs and various environmental variables are explored. The present paper shows novel results regarding HOICs and the relationships between HOICs and dynamic and environmental variables and is suitable for *Atmospheric Measurement Techniques (AMT)*. However, the manuscript includes several insufficient descriptions and a lack of validation of some of the retrieval algorithms used in the present study. This manuscript requires major revisions before reconsideration of publication. Please find the comments below for potential improvements to the manuscript.

Reply: We sincerely thank Referee #1 for reviewing our paper and providing constructive comments for improvement. Responses to these comments are provided below. In this author's comment, we reply (in blue font) to Referee #1's comments (in black font). The relevant part in the revised version is in green font.

Major comment

1. Page 1, Line 3 in abstract and elsewhere "pixel": The terminology "pixel" is often used for a unit of the smallest area in the two-dimensional image data. For example, a satellite pixel indicates the smallest spatial area resolved by spaceborne spectrometers/imagers. It is a bit odd to use the terminology of "pixel" for a measured layer by active-sensor measurements, which is often referred to as a "range". To avoid any unnecessary confusion, I suggest the authors rephrase "pixel" with "range" throughout the text. In addition, a range-resolved algorithm for HOIC detection is not novel but was achieved by many previous studies (e.g., Noel and Sassen, 2005; Stilwell et al., 2019). It may be the first results based on a combination of zenith-pointing and 15° off-zenith pointing lidars, but it would be too specific to claim the first results. I suggest the authors simply remove the statement "for the first time".

Reply: Thank you for the critical comment!
The terminology "pixel" can be seen in other lidar-based literatures like:
Cloudnet related: Hogan and Ewan (2004), Schimmel et al. (2022)
PollyNET: Baars et al. (2017)
EarthCARE: Zadelhoff et al. (2023). Donovan et al. (2024)

➢ To avoid any unnecessary confusion, we have changed the terminology "pixel" to "range", "range bin" or "bin" in different positions. And we have changed "pixel-by-pixel" to "range-resolved".

➢ We have removed the statement "for the first time" both in the abstract and Line 91.

2. On page 7, Lines 195-199, the authors discuss the horizontal deviation of the off-zenith pointing lidar. The discussions tacitly assume that the wind direction is along the line between the scattering volumes of the zenith-pointing and off-zenith-pointing lidars. This is not often the case in reality. The zenith-pointing lidar and off-zenith-pointing lidar often consistently measure a different portion of ice clouds, and therefore the time average does not justify these lidars observing the same portion of clouds. The authors must assume that clouds are horizontally homogeneous over a certain lateral scale, which is a strong assumption. Please clearly state the tacit assumption and discuss the validity of the assumption.

Reply: Thank you for pointing out this. The wind direction is not always along the line between the scattering volumes of the two-angle lidars.

The off-zenith-pointing lidar was pointing towards the due north to avoid the noise of sunlight to the greatest extent. The wind rose plot (wind direction distribution) in Beijing radiosonde station in the whole year of 2022 is shown in Fig. S1. Two kinds of criteria are used to select the height and temperature where HOICs tend to exist: (a) altitude between 4 km and 8 km; (b) temperature between -30 ℃ and -5 ℃. From the wind rose frequency diagram, we found the dominant wind direction over Beijing where HOICs are found is west and northwest, which can also be seen in Fig. 6b.

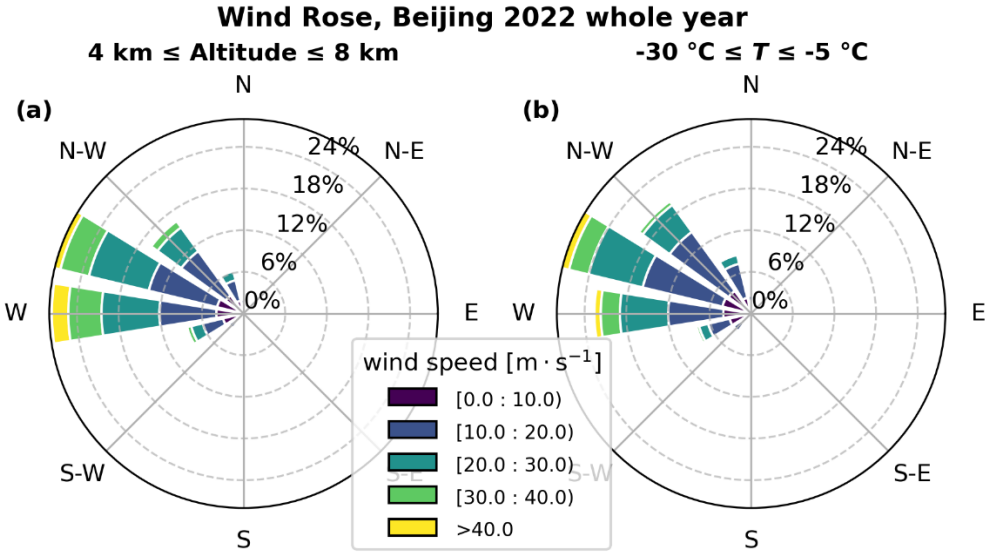

Figure S1. The wind rose plot of Beijing radiosonde station, the whole year 2022. (a) The altitude between 4 km and 8 km was selected. (b) The temperature between -30 ℃ and -5 ℃ was selected. Around 20, 000 radiosonde data points are used to create this plot.

In this way, the wind direction was only sometimes (when the wind vector has a north or south component) along the line between the scattering volumes of the two-angle lidars.

In the revised text, we have clearly added (Lines 197 -205 in the revised manuscript) the assumption of horizontal homogeneity of the clouds, as shown below. This is a strong assumption, and all research based on a two-angle lidar scheme faces this problem (Westbrook et al., 2010; He et al., 2021).

> "Assuming a horizontal wind speed is v = 20 m s^{-1} (see radiosonde Fig. 6b) and the wind direction is along the line between the scattering volumes of the two angle lidars, the horizontal movement of the cloud is 6000 m within five minutes, which is the temporal resolution utilized in data processing. Consequently, if both lidars observe the same cloud within the same time slot (> 5 min), the horizontal deviation of the off-zenith pointing lidar is less significant (1.6 km < 6 km). Although with increasing height, the horizontal distance between the probed volumes also increases (from 0.268 km at 1 km height to 2.68 km at 10 km height.). In reality, the wind direction does not always align with the line connecting the scattering volumes of the two-angle lidars. Therefore, we must assume horizontal homogeneity of the detected cloud layers over a certain lateral scale. This assumption is likely valid for horizontally homogeneous stratiform clouds. However, caution is needed for discrete, small-scale clouds, as misalignment may occur."

3. On page 18, the authors discuss the Euclidean distance from supercooled water clouds to ROICs and HOICs. The motivation behind this analysis is a bit questionable. First of all, the authors should separate the horizontal distances and vertical distances in the analyses as many microphysical processes (e.g., gravitational settling, ice aggregations, etc.) are reflected in the vertical distributions of cloud microphysical properties, and those of horizontal distributions may be influenced by a limited number of physical processes (e.g., turbulence, wind shear, etc.). With this in mind, the present analysis compares the distributions of Euclidean distances between HOICs and ROICs, which will unlikely to provide a meaningful interpretation as the distances in the discussion are an order of 10 km in contrast to the scales of physical processes and scale of turbulence to be generally less than a few km. I suggest the authors remove the entire discussion regarding Euclidean distance.

Reply: Thank you for pointing out this.

We acknowledge the concerns raised by the Reviewer. Our approach was motivated by the intrinsic need to provide a quantitative measure of the linkage between the presence of liquid water and the occurrence of HOIC. So far, earlier studies only qualitatively elaborated about this relationship (e.g., Westbrook et al., 2010). A quantification of an impact of supercooled liquid water on HOIC generation will be of high value for the community as it would provide an important constraint for HOIC-generating conditions. To our opinion, the presented approach to evaluate the Euclidean distance between certain cloud features (in our case the occurrence of HOIC or ROIC) is thus worth to be introduced. In order to motivate the approach better, we introduced further text to the beginning of Section 4.5 (lines 402-411 of the revised manuscript):

"While this attempt is promising based on case studies of well-defined scenarios, such as for ice formation in stratiform supercooled liquid clouds, a statistically comprehensive approach that covers the full variety of cloud types is challenging. One reason is that often the lidar signal is attenuated already within the ice virgae below, so that no signatures of liquid-dominated ice forming layers can be observed. Cloud radar techniques, in turn, are frequently not sensitive enough to detect layers of liquid water. Second reason is, that the ice-forming supercooled liquid water layers might eventually disappear due to cloud dynamical or microphysical processes, while the formed ice particles still exist. A third reason is that vertical wind shear and the microphysical evolution of the ice particles during falling blur the signatures of potential direct relationships between liquid layers and HOIC occurrence.
In here, we introduce the application of the Euclidean distance between supercooled liquid water bins and HOIC or ROIC, respectively, as an approach to quantify the impact of supercooled liquid water on HOIC formation."

In order to consider the concerns raised by the Reviewer, we introduced another short statement to the conclusions section, where it is now emphasized that this approach is only a starting point for more comprehensive future investigations (lines 454-456 of the revised manuscript)

"We see a high potential in using the Euclidean distance approach, even though an improved quantification will require an enhanced characterization of the presence of liquid water beyond lidar attenuation (e.g., Schimmel et al., 2022) and an improved consideration of the ice crystal evolution during sedimentation (Vogl et al., 2024)."

4. Appendix D: The present analyses use the retrieval of ice crystal diameters as described in Appendix D. However, there are no descriptions of the uncertainty and potential bias in the estimated ice crystal diameters. The algorithm relies on a substantially simplified treatment of ice crystal shapes and orientations and is laid upon several approximations (e.g., aspect ratios). The authors should discuss the accuracy of the retrieval method in Appendix D.

Reply: Thank you for pointing out this. We try to analyze the uncertainty of retrieval. This method was widely used in previous studies (Westbrook et al. 2010; He et al. 2021). Three main points are considered as the main primary sources of uncertainty.

1. As you suggested, first we try to change the aspect ratio. Currently, we use the fixed aspect ratio (*h/D*, height divided by diameter) of 0.04 for the hexagonal plate. Now, we do the sensitivity tests for the assumed aspect ratio. Change the aspect ratios for the hexagonal plate from 0.01 to 0.2 (Beard 1980; Stout et al., 2024).

First, we consider a fixed falling velocity of 0.8 ms^{-1}(median Doppler velocity found in this study). Fix the temperature and air pressure condition as of 13 October 2022. The corresponding mean Re and *D* are shown in Table 1, the retrieved Re and *D* are rather sensitive to the assumed fixed aspect ratio.

Table 1. Estimated mean Reynolds number and crystal diameter corresponding to a fall velocity of 0.8 ms^{-1} using a fixed aspect ratio.

Aspect ratio	Re	D [μm]
0.01	102	3041
0.04	**40**	**1207**
0.08	26	779
0.1	23	679
0.2	15	446

To minimize the possible uncertainty introduced by the fixed aspect ratio, instead, we use the dynamic empirical relationships (functions of diameter) used by the previous studies:

Saito et al. (2019)

$$\frac{h}{D} = \left(0.8038\left(\frac{D}{2}\right)^{0.526}\right)^{-1}, D > 10\ (\mu m) \quad (1)$$

Bréon et al. (2004)

$$\frac{h}{D} = 2.01D^{-0.551}\ (\mu m) \quad (2)$$

From Eqs. (D1), (D4) and (D5), we combine Eqs (1) and (2), respectively. The estimated Reynolds number and crystal diameters are calculated and shown in Table 2.

Table 2. Estimated mean Reynolds number and crystal diameter corresponding to a fall velocity of 0.8 ms^{-1} using different empirical aspect ratio relationships.

Empirical *h/D* relationship	Calculated Aspect ratio	Re	*D* [μm]
Saito et al., 2019	0.044	38	1129
Bréon et al., 2004	0.043	40	1199

The corresponding retrieved Re and *D* are quite close to the results using the fixed aspect ratio of 0.04, which confirms the validity of using a fixed aspect ratio of 0.04.

Next, instead of using a fixed median falling velocity, we use the real detected Doppler velocity (a distribution of velocity with a median value of 0.8 ms^{-1}), the corresponding distribution and statistics of Re and *D* are shown below in Fig. S2 and Table 3:

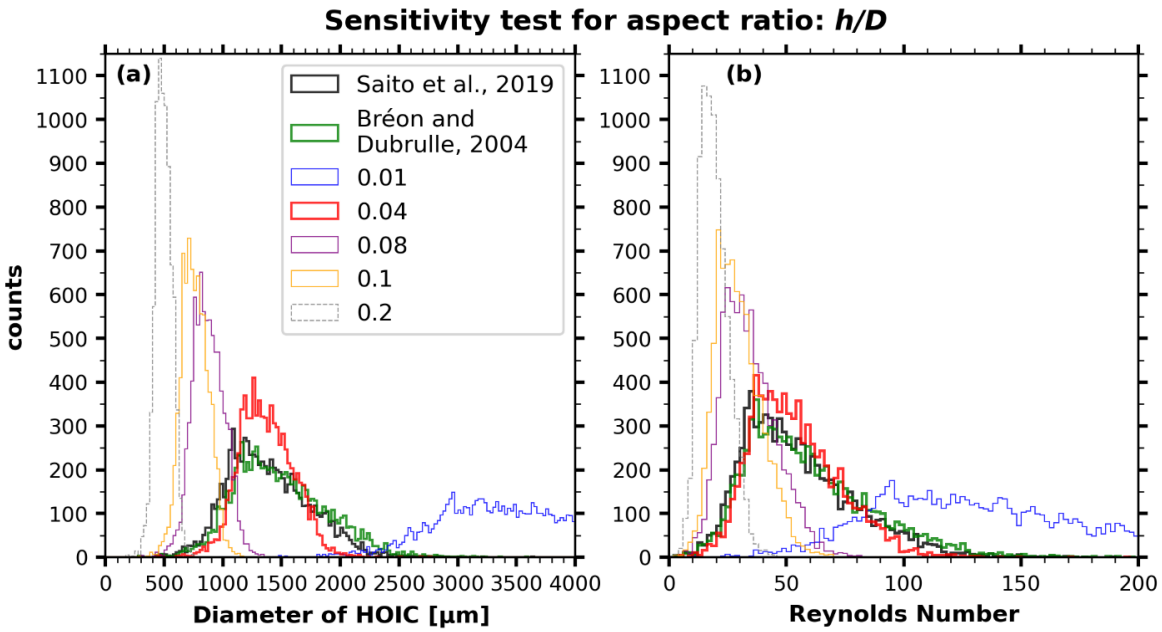

Figure S2. (a) The histogram of retrieved diameters of HOICs. (b) The histogram of retrieved Reynolds numbers of HOICs. Dynamic empirical relationships and fixed different aspect ratios (from 0.01 to 0.2) are used for *D* and *Re* retrievals.

Table 3. Different aspect ratios: statistics of estimated diameter and Reynolds number for HOICs on 13 October 2022.

Aspect ratio	Statistics	Re	*D* [μm]
0.04	5th percentile	28	1029
	First quartile	39	1204
	Median	51	1354
	Third quartile	65	1525
	95th percentile	88	1756
	Mean	54	1369
Saito et al., 2019	5th percentile	24	894
	First quartile	37	1125
	Median	50	1342
	Third quartile	69	1611
	95th percentile	101	2016
	Mean	55	1387
Bréon et al., 2004	5th percentile	26	941
	First quartile	39	1194
	Median	54	1434
	Third quartile	74	1735
	95th percentile	110	2193
	Mean	59	1487

From Fig. S2 and Table 3, we can conclude that using a fixed aspect ratio of 0.04 leads to limited uncertainty compared to the empirical aspect ratio relationships used in literature (Bréon et al., 2004; Saito et al., 2019). The median and mean retrieved diameters and Reynolds numbers obtained with the fixed aspect ratio of 0.04 are particularly close to those derived from Saito et al. (2019)'s empirical dynamic relationships. The only notable difference is that the distributions of Re and *D* from the dynamic relationship are wider.

2. The shape of the particle also contributes to the uncertainty of the retrieval. The hexagonal plate is the most simplified shape, widely used for oriented ice (Bréon et al., 2004; Zhou et al., 2012; He et al., 2021). As Westbrook et al. (2010) have already shown in their Table III. The crystal diameter corresponding to a certain falling velocity is rather sensitive to the assumed shape of ice crystals. To make it concise and comparable to the previous research, we kept using hexagonal plates.

3. The assumption that Doppler velocity represents the terminal velocity of a particle is a rough approximation. However, in general, long-term measured Doppler velocity can partially mitigate the effect of rapidly changing vertical airflow and provide an approximate still-air velocity for falling ice crystals. A reasonable approach to reducing uncertainty is to remove extreme values from the retrieved Reynolds numbers and diameters. Therefore, we focus on the intermediate range of the retrieved diameters and Reynolds numbers, excluding extreme values (e.g., data points beyond the 5th and 95th percentiles).

We have added a discussion part about the uncertainty in Appendix D in terms of the above three points:

"After conducting careful sensitivity tests, we found that the assumed fixed aspect ratio of 0.04 yields a retrieved diameter and Reynolds number similar to those obtained using empirical dynamic aspect ratio relationships reported in the literature (Bréon et al., 2004; Saito et al., 2019). It is important to note that crystal diameter and Reynolds number are highly sensitive to the shape of ice crystals (Westbrook et al., 2010, Table III). The assumed HOIC shape of hexagonal plates is the most simplified and widely used model (Bréon et al., 2004; Zhou et al., 2012; He et al., 2021). Additionally, assuming that Doppler velocity represents the terminal velocity of a particle in still air introduces some uncertainty. However, in general, long-term Doppler velocity measurements can partially mitigate the effect of rapidly changing vertical airflow and provide an approximate still-air velocity for falling ice crystals. To reduce the potential uncertainty caused by extreme vertical airflow, we focus only on the intermediate range of the retrieved diameters and Reynolds numbers, excluding extreme values (e.g., data points beyond the 5th and 95th percentiles). In summary, this method serves as an estimation to compare the case with previous studies (Westbrook et al., 2010; He et al., 2021a)."

Minor comments

1. Page 2, Lines 31-32 "Mie scattering …": Mie scattering theory applies to spheres and cannot examine the differences in the scattering cross-sections between random orientation and preferential orientations (i.e., particle orientations cannot be defined). Please clarify the point of the statement.

   Reply: Thank you for pointing out this! This viewpoint is originally from the penultimate paragraph of Várnai et al. (2019).
   We have rephased the sentence in terms of this by removing the "Mie scattering":

   "Calculation shows oriented plates intercept roughly twice as much sunlight as the perfectly randomly oriented ones (Várnai et al., 2019)."

2. Page 3, Line 60: "didn't" should be "did not".

   Reply: Done.

3. Page 3, Lines 71-72: "Westbrook et al. 2010" Suggest the authors add "Sato and Okamoto (2011)."

   Reply: Done. We have added Sato and Okamoto (2011).

4. Page 3, Line 72: "Zhou et al., 2012a" Suggest the authors add "Saito et al., (2017)."

   Reply: Done. We have added Saito et al., (2017).

5. Page 5, Line 123 "cos(75°)": It would be better to use a unit of steradian inside the cosine. By the way, should this be 15°? Cos(15°) is a very small value.

   Reply: Thank you for pointing out this. It should be 15° or $\frac{\pi}{12}$ in the unit of steradian. We used $\cos\left(\frac{\pi}{12}\right)$ in Line 123. And we also used $\tan\left(\frac{\pi}{12}\right)$ in Line 195.

6. Page 13, Lines 307-309 "… the strong turbulence caused by the latent heat released due to the sublimation…": This statement lacks supporting evidence and is not beyond the speculation level. Please provide sufficient evidence supporting this or clearly state that this is based on the authors' speculation.

   Reply: This is from the authors' speculation. We have clearly stated this in the revised version Line 314-316:

   "The high δ_v region above the cloud base (Fig. 5b, brown line within the red shaded region, also see Fig. 4d) in the zenith lidar observation appears to be associated with

a higher eddy dissipation rate (Fig. 5e, also see Fig. 4j), suggesting that the strong turbulence may be linked to latent heat release from the sublimation of ice crystals near the cloud base."

7. Page 15, Line 334 "A negative correlation is found …": Is there a hypothesized mechanism for the negative correlation? Also, is this true for ROICs or not?

Reply: Overall, within the troposphere, the higher the altitude, the lower the temperature, and the higher the horizontal wind speed. The horizontal wind and the temperature are negatively correlated. The description here is to confirm the negative correlation relationship for the environment variable of HOICs. That is also true for ROICs, as shown in Fig. S3 below:

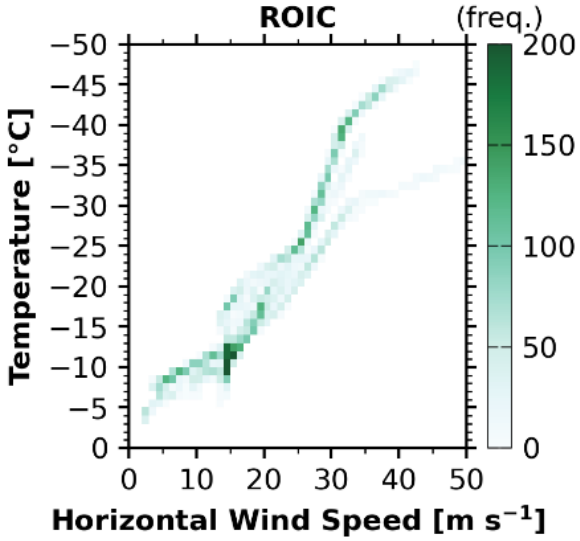

Figure S3. The density scatter plot of horizontal wind speed and temperature where ROICs exist, the greener the color, the higher the number density of ROIC pixels

8. Figure 4 and Page 18, Line 370: I am concerned with the consistency of the scattering volumes between radar and lidars. Between 16:00 and 18:00 in Fig. 4, the liquid layer appears at an altitude of 5-6 km, as evidenced by the strong echoes from both lidars. However, it is not seen from radar. Please discuss the scattering volume consistencies. Perhaps the authors need to discuss the minimum detectable radar reflectivity in Section 2.4.

Reply: Yes, the minimum detectable radar reflectivity is about -40 dBZ. Some small supercooled liquid water droplets are too small, they can be detected by the lidars and are not detectable by radar (especially for the Ka-band radars compared with W-band radars which have a shorter wavelength and are more sensitive to smaller particles).

We have added the discussion of the scattering volume consistencies on Page 18, Line 399-400:

"It should be noted that the scattering volume of lidars and radar is not exactly the same. Small liquid droplets and optically thin ice clouds are sometimes not detectable from Ka-band radar compared with lidars."

`

We have added the minimum detectable radar reflectivity discussion in Section 2.4.

"The minimum detectable reflectivity factor of this radar is -40 dBZ. Compared to lidars, radar exhibits greater sensitivity to larger particles (Westbrook et al., 2010; Bian et al., 2023). However, this Ka-band cloud radar may fail to detect certain tiny liquid droplets and optically thin ice clouds."

9. Figure 4 and Page 18, Lines 375–376 "… the signals of both lidar systems were subject to strong attenuation": It is hard to see the attenuation from Fig. 4 which uses a linear scale in the attenuated backscattering coefficients. Suggest the authors use a log scale in this figure.

Reply: Thank you for pointing out this. We have changed Figs.4a and 4c (Fig. S4 below) to log scale to show the attenuation in the revised manuscript.

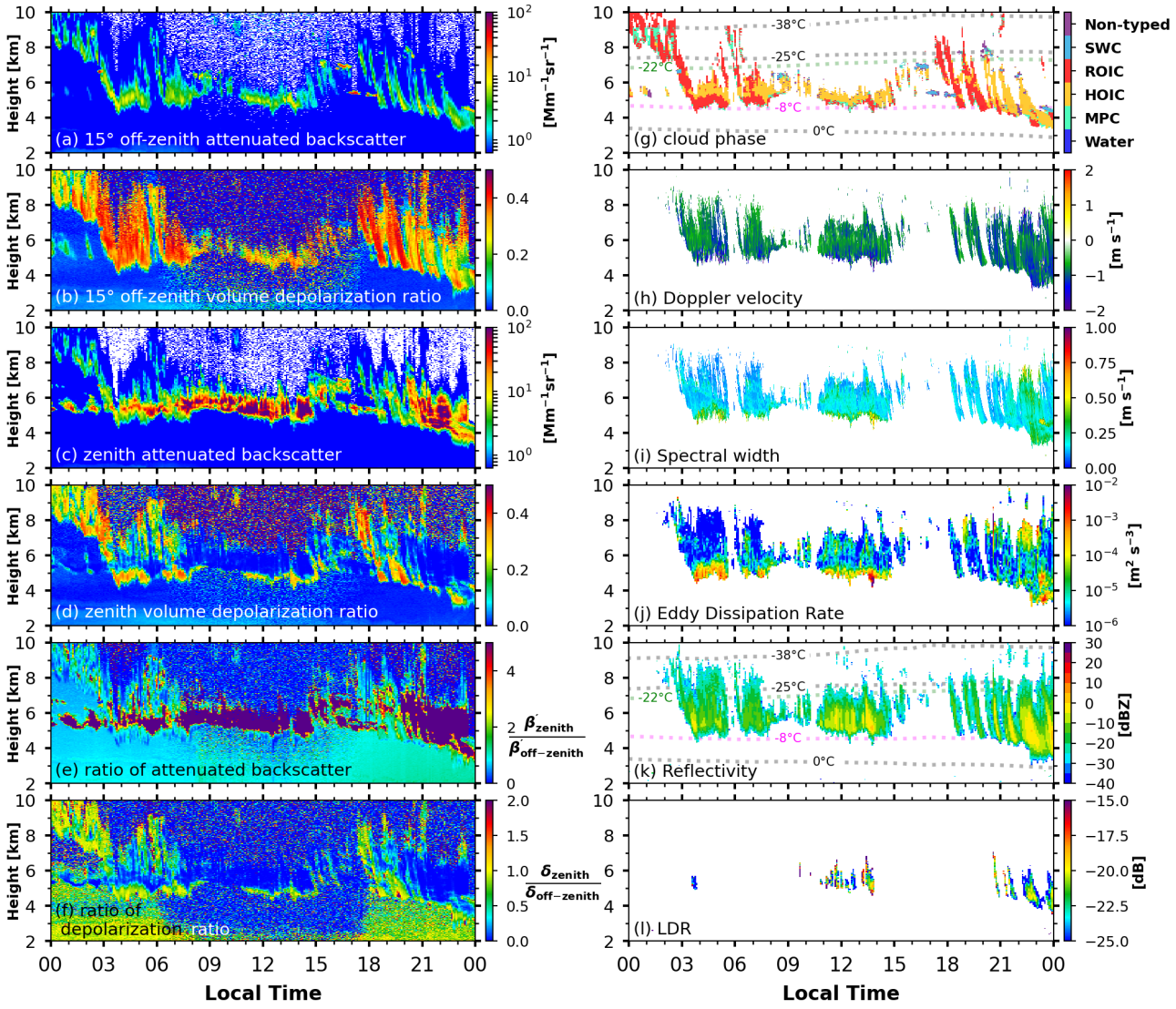

Figure S4. Lidar ((a)-(g)) and zenith-pointing Ka-band cloud radar ((h)-(l)) observations on 13 October 2022, time-height contour plots (5 min / 15 m resolution for (a)-(g), 13 s / 30 m resolution for (h)(i) to show the variation of Doppler velocity, 5 min / 30 m for (j)-(l)). (a) 15 ◦ off-zenith-pointing lidar attenuated backscatter. (b) 15 ◦ off-zenith-pointing lidar volume depolarization ratio. (c) Zenith-pointing lidar attenuated backscatter. (d) Zenith-pointing lidar volume depolarization ratio. (e) The ratio of attenuated backscatter for zenith-pointing and off-zenith-pointing lidar. (f) The ratio of volume depolarization ratio for zenith-pointing and off-zenith-pointing lidar. (g) Cloud phase categorization results with isotherm from ERA 5 data. Abbreviations of SWC, ROIC, HOIC, and MPC represent supercooled liquid water cloud, randomly oriented ice crystal, horizontally oriented ice crystal, and mixed-phased cloud. There is no cloud pixel categorized as (warm) water due to the subzero temperature. (h)(i)(k)(l) Cloud radar detected momentum data: Doppler velocity, spectral width, reflectivity (with isotherm from ERA 5 data), and linear depolarization ratio (LDR). (j) Cloud radar retrieved eddy dissipation rate (EDR, ϵ).

Reference

Baars, H., Seifert, P., Engelmann, R., and Wandinger, U.: Target categorization of aerosol and clouds by continuous multiwavelength-polarization lidar measurements, *Atmos. Meas. Tech., 10*, 3175–3201, https://doi.org/10.5194/amt-10-3175-2017, 2017.

Beard, K. V.: The Effects of Altitude and Electrical Force on the Terminal Velocity of Hydrometeors. *J. Atmos. Sci.*, **37**, 1363–1374, https://doi.org/10.1175/1520-0469(1980)037<1363:TEOAAE>2.0.CO;2, 1980.

Bian, Y., Liu, L., Zheng, J., Wu, S., & Dai, G: Classification of cloud phase using combined ground-based polarization LiDAR and millimeter cloud radar observations over the Tibetan Plateau. *IEEE Transactions on Geoscience and Remote Sensing*, *61*, 1-13, https://doi.org/10.1109/LGRS.2019.2930866, 2023

Bréon, F.-M. and Dubrulle, B.: Horizontally oriented plates in clouds, *Journal of the atmospheric sciences, 61*, 2888–2898, https://doi.org/10.1175/JAS-3309.1, 2004.

Donovan, D. P., van Zadelhoff, G.-J., and Wang, P.: The EarthCARE lidar cloud and aerosol profile processor (A-PRO): the A-AER, A-EBD, A-TC, and A-ICE products, Atmos. Meas. Tech., 17, 5301–5340, https://doi.org/10.5194/amt-17-5301-2024, 2024.

He, Y., Liu, F., Yin, Z., Zhang, Y., Zhan, Y., and Yi, F.: Horizontally oriented ice crystals observed by the synergy of zenith-and slant-pointed polarization lidar over Wuhan (30.5° N, 114.4° E), China, *Journal of Quantitative Spectroscopy and Radiative Transfer, 268,* 107 626, 675 https://doi.org/10.1016/j.jqsrt.2021.107626, 2021.

Hogan, Robin J., and Ewan J. O'Connor. Facilitating cloud radar and lidar algorithms: the Cloudnet Instrument Synergy/Target Categorization product. *Cloudnet documentation* 14, 2004.

Saito, M. and Yang, P.: Oriented ice crystals: a single-scattering property database for applications to lidar and optical phenomenon simulations, *Journal of the Atmospheric Sciences, 76*, 2635–2652, https://doi.org/10.1175/JAS-D-19-0031.1, 2019

Schimmel, W., Kalesse-Los, H., Maahn, M., Vogl, T., Foth, A., Garfias, P. S., and Seifert, P.: Identifying cloud droplets beyond lidar attenuation from vertically pointing cloud radar observations using artificial neural networks, *Atmos. Meas. Tech., 15*, 5343–5366, https://doi.org/10.5194/amt-15-5343-2022, 2022.

Stout, J. R., Westbrook, C. D., Stein, T. H. M., and McCorquodale, M. W.: Stable and unstable fall motions of plate-like ice crystal analogues, *Atmos. Chem. Phys., 24,* 11133–11155, https://doi.org/10.5194/acp-24-11133-2024, 2024.

van Zadelhoff, G.-J., Donovan, D. P., and Wang, P.: Detection of aerosol and cloud features for the EarthCARE atmospheric lidar (ATLID): the ATLID FeatureMask (A-FM) product, *Atmos. Meas. Tech., 16*, 3631–3651, https://doi.org/10.5194/amt-16-3631-2023, 2023.

Várnai, T., Kostinski, A. B., and Marshak, A.: Deep space observations of sun glints from marine ice clouds, *IEEE Geoscience and Remote Sensing Letters, 17*, 735–739, https://doi.org/10.1109/LGRS.2019.2930866, 2019

Westbrook, C., Illingworth, A., O'Connor, E., and Hogan, R.: Doppler lidar measurements of oriented planar ice crystals falling from supercooled and glaciated layer clouds, *Quarterly Journal of the Royal Meteorological Society, 136*, 260–276, https://doi.org/10.1002/qj.528, 2010.

Zhou, C., Yang, P., Dessler, A. E., and Liang, F.: Statistical properties of horizontally oriented plates in optically thick clouds from satellite observations, IEEE Geoscience and Remote Sensing Letters, 10, 986–990, https://doi.org/10.1175/JAMC-D-11-0265.1, 2012